The Effect of Varying Stratification on Low-Frequency Equatorial Motions

ANTONIO J. BUSALACCHI

Laboratory for Oceans, NASA/Goddard Space Flight Center, Greenbelt, Maryland

MARK A. CANE

Lamont-Doherty Geological Observatory of Columbia University, Palisades, New York

(Manuscript received 12 May 1987, in final form 18 November 1987)

ABSTRACT

A formalism is developed to examine the effect of zonally varying stratification on equatorial wave phenomena; an effect present in the real ocean but neglected from standard linear theory. The approach utilized involves the application of a matching condition to equatorial waves incident on a single zonal discontinuity in the density field of a shallow water system. Transmission and reflection coefficients are sought for the projection of an incoming wave onto the entire set of resultant vertical and horizontal wave modes of a general continuously stratified fluid. The limiting case of a meridional density front is extended, in a manner analogous to radiative transfer problems, to a series of discrete density intervals. These techniques are applied to specific choices of stratification ranging from a zonal jump discontinuity in the density field to density changes with zonal scales large with respect to the waves in question, i.e., a WKB limit. The results demonstrate that zonally varying stratification does not produce substantial changes in the energy flux of propagating equatorial waves. However, as a result of changes to the equatorial radius of deformation, the amplification of equatorial zonal velocity can be appreciable. A corresponding decrease in pressure, albeit smaller, may also be non-negligible.

1. Introduction

One of the common approaches to the study of equatorial ocean circulation has been to invoke linear theory. Problems in this class include the steady vertical structure of equatorial currents, the seasonal response in each tropical ocean, and interannual events such as El Niño. Those studies that include nonlinear physics often utilize linear equatorial wave theory to decipher the more complicated solutions. By necessity or for simplicity these approaches tend to neglect effects due to coastal geometry, islands, bottom topography, or spatial and temporal variations in the stratification of the ocean.

Previous investigations have addressed the influence of several of these effects on equatorial waves. Clarke (1983) and Cane and Gent (1983) considered the reflection of equatorial waves from non-meridional eastern and western boundaries. Yoon (1981), Cane and du Penhoat (1982) and Rowlands (1982) calculated the effects of islands on equatorial wave motions. The influence of submarine ridges was recently considered by McPhaden and Gill (1986). Yet to be addressed is the influence of horizontal variations in stratification.

The standard procedure in linear theoretical studies is to linearize about a basic state including the assumption that the vertical stratification is horizontally uniform. Together with assumptions on vertical and horizontal mixing, this permits the vertical dependency to be separable from the horizontal and temporal structure. The vertical structure is decomposed into an infinite series of vertical normal modes corresponding to eigenfunctions of a Sturm-Liouville equation. The associated eigenvalues determine the phase speed, or equivalently the deformation radius of each mode. All of these are fixed in space and time.

Hydrographic observations indicate, however, a rich structure to the density field at low latitudes. The most prominent feature is the zonal slope of the equatorial thermal field. In response to mean easterly trade winds, the equatorial thermocline shoals eastward by approximately 160 m across the Pacific Ocean (Meyers 1979) and 100 m across the Atlantic Ocean (Merle 1980). In both oceans the change is comparable to the mean depth. On a smaller spatial scale, associated with the oblique intersection of the Galapagos Front and the equator, mean dynamic height (0/500 db) changes 5 dyn cm in a zonal distance of 300 km in the eastern equatorial Pacific: This change in dynamic height is roughly one-half the amplitude of the seasonal cycle (Lukas 1981). Representative of these zonal changes is the range in baroclinic phase speeds: computations using CTD observations at 179°W have indicated phase speeds of 291 and 178 cm s^{-1} for first and second baroclinic modes (Eriksen et al. 1983); in contrast, the mean

Corresponding author address: Dr. Antonio Busalacchi, Code 671, Goddard Space Flight Center, Greenbelt, MD 20771.

density profile at 92°W yields speeds of 214 and 111 cm s^{-1} for the first two modes (Lukas 1981).

An extreme example of temporal changes is the 100 m isopycnal displacement observed on the equator at 85°W during the 1982 El Niño (Behringer 1984). In the context of a two-layer system with $\Delta\rho/\rho = 2 \times 10^{-3}$ and initial pycnocline depth of 200 m, a 100 m pycnocline displacement would correspond to a change in phase speed from 200 to 245 cm s^{-1}.

Variations of the density field such as these, and the inherent changes in the deformation scaling, lead us to question their importance for equatorial wave dynamics. Examples of interest include the behavior of equatorial waves impinging upon a meridionally oriented density front and waves propagating along a sloping thermocline. One potential application is to the question of whether the response to wind energy input in the western equatorial Pacific retains its modal identity eastward or is transformed and depleted through significant modal dispersion.

The intent of this work is to develop a formalism to examine the influence of zonally varying stratification on equatorial wave phenomena, and subsequently illustrate the application to idealized cases. We wish to isolate the influence of zonal changes in stratification; mean currents are ignored. Our work is thus complementary to that of McPhaden et al. (1986), which neglects zonal variations but treats the influence of mean currents and the associated meridional variations in stratification required for geostrophic balance. We are aware of the inconsistency in the present approach: a basic state with a horizontally varying stratification generates non-zero pressure gradient forces which presumably are balanced by forces associated with water motion. There is general agreement that stresses associated with zonal currents are important to the zonal momentum balance, but there is no universally accepted idea of what form these stresses take. Consequently, there is no obvious choice for the currents associated with a zonal pressure gradient. Rather than becoming enmeshed in this issue, and in efforts to separate the influence of mean currents from that of stratification per se, we simply assume ab initio that mean currents may be neglected.

Our approach, as described in sections 2 and 3, is to apply a matching condition to equatorial waves incident on a single zonal discontinuity in the density field of a shallow water system. Transmission and reflection coefficients are sought for the projection of the incoming wave onto the entire set of resultant vertical and horizontal wave modes of a general continuously stratified fluid. In contrast to a WKB procedure this approach allows us to examine the cases where the density variations are rapid compared to the wavelength. For the long waves of greatest interest in low-frequency equatorial dynamics this is the more realistic limit. This is extended in section 4, in a manner analogous to radiative transfer problems, to a finite number of discrete density intervals. In section 5 these techniques are implemented for specific choices of stratification. The results are summarized and the implications are discussed in the final section.

2. Equatorial Kelvin wave incident on a meridional density front

We first consider a low-frequency, free equatorial Kelvin wave with time dependence $\exp(i\omega t)$ incident on a discrete change in the vertical stratification at $x = 0$. The ocean is unbounded, and the density fields within the regions east and west of the discontinuity are horizontally homogeneous: west of $x = 0$ the Brunt–Väisälä frequency is $N(z)$; east of $x = 0$ it is $N'(z)$. (We will use primes to mark variables east of $x = 0$.) The usual decomposition into vertically standing modes (e.g., Moore and Philander 1977) results in a set of structure functions and associated wave speeds $\{F_m(z), C_m, m = 1, 2, \cdots\}$ west of the front which differs from the set $\{F'_m(z), C'_m, m = 1, 2, \cdots\}$ east of it. As a result the incident free Kelvin wave, with vertical index I and structure $F_I(z)$, cannot pass through $x = 0$ unaltered.

It is intuitive, as well as straightforward to demonstrate rigorously, that zonal velocity u and dynamic pressure p must be continuous across the interface $x = 0$. Since this is true for all t, all motions generated by the incident Kelvin wave must also have the form $\exp(i\omega t)$. The solution may be considered to be composed entirely of free waves at the low frequency ω. We first list the possible components and establish notation. (The notation is the dimensional version of that used in Cane and Sarachik 1981, henceforth CS.)

(i) The incident Kelvin wave, with unit amplitude at $x = 0$:

$$(u, p) = 2^{-1/2}\psi_0(y_I)e^{-ix_I}(C_I, C_I^2)F_I(z)$$

$$\equiv \mathbf{K}_I(y_I)e^{-ix_I}F_I(z); \quad (2.1)$$

where

$$x_I = \omega x/C_I; \quad y_I = y/L_I, \quad (2.2)$$

$$\psi_0(y) = \pi^{-1/4}e^{-1/2y^2} \quad (2.3)$$

is the zero-order Hermite function, and $L_I = (C_I/\beta)^{1/2}$ is the equatorial radius of deformation for vertical mode I. This Kelvin wave is present only west of the front; i.e., for $x < 0$.

(ii) An infinite number of long Rossby waves reflected at $x = 0$ and propagating westward in the region $x < 0$. The sum of these waves may be written in the form

$$(u, p) = \sum_{m=1}^{\infty} \mathbf{S}_m(x_m, y_m)F_m(z), \quad (2.4)$$

where $x_m = \omega x/C_m$ and $y_m = y/L_m$. For each vertical mode m, $\mathbf{S}_m$ is composed of an infinite sum of long Rossby waves with different meridional structure, but

for the present we need not concern ourselves with this additional decomposition.

(iii) An infinite number of transmitted Kelvin waves with amplitude T_m propagating eastward east of the front ($x > 0$):

$$(u, p) = \sum_{m=1}^{\infty} T_m \mathbf{K}'_m(y'_m) e^{-ix'_m} F'_m(z). \quad (2.5)$$

The notation is analogous to (2.1)ff.

(iv) Transmitted, short Rossby waves east of $x = 0$. At $x = 0$

$$(u, p) = \sum_{m=1}^{\infty} (C'_m X_m{}^u(y'_m), C'^2_m X_m{}^p(y'_m)) F'_m(z)$$

$$= \sum_{m=1}^{\infty} \mathbf{X}'_m F'_m(z). \quad (2.6)$$

Our method of solution is an extension of the methods of CS and is similar to the technique used by Cane and DuPenhoat (1982) to solve for the flow past equatorial islands. In the notation of (2.1)–(2.6) the condition that u and p be continuous at $x = 0$ for all y becomes

$$\mathbf{K}_I F_I + \sum_{m=1}^{\infty} \mathbf{S}_m (x = 0) F_m = \sum_{m=1}^{\infty} T_m \mathbf{K}'_m F'_m + \sum_{m=1}^{\infty} \mathbf{X}'_m F'_m. \quad (2.7)$$

In practice the infinite sums in (2.7) are truncated at some finite upper limit M. Although it is not strictly necessary to do so in order for our analysis to proceed, doing so now avoids certain technical questions related to convergence. We continue in a manner analogous to Cane and DuPenhoat (1982). The equatorial Kelvin waves have $v = 0$ and in the low frequency limit the long westward Rossby waves also have $v \approx 0$. Hence the lhs of (2.7) and the Kelvin waves on the rhs all satisfy the geostrophic relation

$$\beta y u + \partial p / \partial y = 0. \quad (2.8)$$

It follows that the short Rossby waves must also satisfy this relation for each m (since the F'_m are mutually orthogonal). Cane and Sarachik (1977) show that in the low frequency limit there is a streamfunction $\Psi(y'_m)$ such that

$$X_m{}^u = -\partial \Psi / \partial y'_m; \quad X_m{}^p = y'_m \Psi.$$

Substituting in (2.8), after replacing y by $L'_m y'_m$

$$-\beta L'_m C'_m y'_m \frac{\partial \Psi}{\partial y'_m} + \frac{1}{L'_m} \frac{\partial}{\partial y'_m} [C'^2_m y'_m \Psi] = 0,$$

so

$$-y'_m \partial \Psi / \partial y'_m + \frac{\partial}{\partial y'_m} [y'_m \Psi] = 0.$$

Therefore, $\Psi = 0$ and no short Rossby waves are generated: $\mathbf{X}'_m = 0$.

Returning to the now simpler (2.7) we note that

$$\int_{-D}^{0} F_m F_n dz = \int_{-D}^{0} F'_m F'_n = \delta_{m,n}. \quad (2.9a)$$

Define

$$\gamma_{m,n} \equiv \int_{-D}^{0} F_m F'_n dz \quad (2.9b)$$

and project (2.7) onto the vertical structure function F_j. This eliminates the vertical dependence in (2.7):

$$\mathbf{K}_I \delta_{I,j} + \mathbf{S}_j = \sum_{m=1}^{M} T_m \gamma_{j,m} \mathbf{K}'_m; \quad j = 1, M. \quad (2.10)$$

We now define the dot product scaled from the west side:

$$[(u_m, p_m) \cdot (u'_n, p'_n)]_m \equiv (L_m{}^{-1} C_m{}^{-4}) \times \int_{-\infty}^{\infty} dy [C_m{}^2 u_m u'_n + p_m p'_n], \quad (2.11)$$

with the understanding that the primes are optional. Taking the dot product of (2.10) with $\mathbf{K}_j$ eliminates the Rossby wave term $\mathbf{S}_j$ because the Kelvin wave is orthogonal to each of the Rossby waves in the sum; the result is

$$\delta_{I,j} = \sum_{m=1}^{M} T_m \gamma_{j,m} \kappa_{j,m}, \quad j = 1, M \quad (2.12)$$

where

$$\kappa_{j,m} \equiv [\mathbf{K}_j \cdot \mathbf{K}'_m]_j = 2^{-1/2} \frac{C'_m}{C_j} \left[1 + \frac{C'_m}{C_j}\right] \times \frac{1}{L_j} \left[\frac{1}{L_j^2} + \frac{1}{L'^2_m}\right]^{-1/2};$$

$$\kappa_{j,m} = \mu^{-2} [(1 + \mu)/2]^{1/2} \quad (2.13)$$

with

$$\mu(j, m) = C_j / C'_m = (L_j / L'_m)^2. \quad (2.14)$$

The M unknown transmitted Kelvin wave amplitudes T_m can now be calculated from the M equations (2.12). The rhs of (2.10) is now known so $\mathbf{S}_j$ is now known at $x = 0$. To find its x-dependence for $x < 0$ we may proceed as follows. Since it is a sum of long Rossby waves,

$$\mathbf{S}_j(x_j, y_j) = \sum_{n=1}^{\infty} s_n [C_j R_n{}^u(y_j), C_j^2 R_n{}^p(y_j)] \times \exp[i(2n + 1)x_j], \quad (2.15)$$

where the R are the (u, p) components defined in CS, Eq. (A6). The s_n may be found by projecting the nth Rossby horizontal mode onto (2.10), making use of the orthogonality of the individual Rossby wave terms in (2.15). Only the symmetric (odd n) modes are nonzero.

There is a shortcut to a closed form solution instead of the infinite sum of (2.15). Each term on the rhs of (2.10) has the same Gaussian form and may be rewritten in terms of y_j and C_j as

$$\mathbf{K}'_m = 2^{-1/2}\pi^{-1/4}\mu^{-2}(C_j\mu, C_j^2)\exp[-1/2\mu y_j^2]. \quad (2.16)$$

A sum of free Rossby waves having the form (2.16) at $x = 0$ can be deduced immediately from Eq. (A27) of CS to be

$$\mu^{-2}\left(\frac{1-\mu}{2}\right)^{1/2}\left\{-\left(\frac{1+\mu}{1-\mu}\right)^{1/2}e^{-ix_j}\mathbf{K}_j + e^{ix_j}\mathbf{L}_j\left(y_j, \left[\frac{1-\mu}{1+\mu}\right]^{1/2}e^{2ix_j}\right)\right\} \quad (2.17a)$$

where

$$\mathbf{L}_j(y, \eta) = 2^{-1/2}\pi^{-1/4}\eta^{-1}(1+\eta^2)^{-1/2}((1-\eta^2)C_j, (1+\eta^2)C_j^2)\exp\left[\frac{y^2}{2}\frac{(\eta^2-1)}{(\eta^2+1)}\right]. \quad (2.17b)$$

3. Long Rossby waves incident on a meridional density front

Next we consider a set of low-frequency long Rossby waves impinging on the front at $x = 0$ from the east. At $x = 0$ the waves are assumed to have the form $\mathbf{S}'_I(y)F'_I(z)$. The wave modes available for reflection and transmission are as in (2.2)–(2.4): (i) Long Rossby waves west of $x = 0$; (ii) Kelvin waves east of $x = 0$; (iii) short Rossby waves east of $x = 0$. Since Kelvin waves propagate eastward, none can be generated west of the front. As before [(2.8)ff] the fact that all other terms have u and p in geostrophic balance means the short Rossby waves (iii) cannot be present. Hence the conditions that u and p be continuous across $x = 0$ is, in analogy to (2.7),

$$\sum_{m=1}^{M}\mathbf{S}_m F_m = \sum_{m=1}^{M} T_m\mathbf{K}'_m F'_m + \mathbf{S}'_I F'_I. \quad (3.1)$$

We proceed exactly as before. First, eliminate the vertical dependence by projecting (3.1) onto $F_j(z)$:

$$\mathbf{S}_j = \sum_{m=1}^{M} T_m\gamma_{j,m}\mathbf{K}'_m + \gamma_{j,I}\mathbf{S}'_I, \quad j = 1, M. \quad (3.2)$$

Next, take the dot product of (3.2) with $\mathbf{K}_j$. Since the Rossby waves $\mathbf{S}_j$ are orthogonal to this Kelvin wave,

$$0 = \sum_{m=1}^{M} T_m\gamma_{j,m}\kappa_{j,m} + \gamma_{j,I}[\mathbf{K}_j\cdot\mathbf{S}'_I]_j, \quad j = 1, M. \quad (3.3)$$

Since $\mathbf{S}'_I$ is given, the dot product in (3.3) may be calculated and the M equations (3.3) solved for the unknown amplitudes T_m of the reflected Kelvin waves. The transmitted Rossby waves are now known at $x = 0$ from (3.2). In general, determining their form for $x < 0$ requires writing $\mathbf{S}_j$ as a sum of individual waves as in (2.15) and then finding the amplitude of each by projecting the wave form onto $\mathbf{S}_j$.

4. Multiple changes in the zonal density field

The results of sections 2 and 3 form the basis for considering a multiple number of density intervals. We begin with two discrete changes in density and consider a Kelvin wave incident on the interface J between regions J and $J + 1$ and a Rossby wave incident on the interface between regions $J + 1$ and $J + 2$ (Fig. 1). We set out to solve for the resulting Kelvin wave incident on interface $J + 1$ and the Rossby wave at J. The solution is determined by the transmission and reflection processes outlined in the previous sections together with the internal reflections that take place between the two interfaces. The reflection, transmission, and propagation of the Kelvin and Rossby modes is described by the following operators:

S_J reflection of a Kelvin wave at interface J
T_J transmission of a Kelvin wave at interface J
Q_J reflection of a Rossby wave at interface J
U_J transmission of a Rossby wave at interface J
P_J^K Kelvin wave propagation across region J
P_J^R Rossby wave propagation across region J.

The Kelvin wave, K_J, incident on interface J will produce a reflected Rossby response in region J and a transmitted Kelvin disturbance in region $J + 1$. In a similar manner the Rossby wave, R_{J+1}, incident on interface $J + 1$ will reflect as Kelvin waves in region $J + 2$ and transmit Rossby waves to region $J + 1$. Within region $J + 1$ the transmitted waves undergo multiple reflections between interfaces J and $J + 1$.

The problem described above is analogous to the discrete difference approach to the equation of radiative transfer for a slab of some medium (Peebles and Plesset 1951; Grant and Hunt 1968). Our approach follows accordingly.

We seek to calculate the transitions in region $J + 1$ from interface J to interface $J + 1$. The reader will find

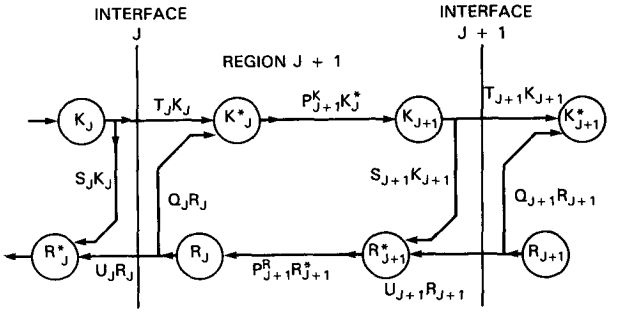

FIG. 1. Schematic of the reflection and transmission processes between two discrete changes in density.

it helpful to refer to Fig. 1. Propagation of wave forms across region $J+1$ is characterized as

$$K_{J+1} = P^K_{J+1} K^*_J, \tag{4.1a}$$

$$R_J = P^R_{J+1} R^*_{J+1}. \tag{4.1b}$$

The Kelvin wave on the eastern side of interface J, K^*_J is a combination of transmitted and reflected Kelvin waves. The Rossby wave on the western side of $J+1$, R^*_{J+1} is a combination of transmitted and reflected Rossby waves, i.e.,

$$K^*_J = T_J K_J + Q_J R_J, \tag{4.2a}$$

$$R^*_{J+1} = S_{J+1} K_{J+1} + U_{J+1} R_{J+1}. \tag{4.2b}$$

Eliminating the starred terms relates waves about to exit region $J+1$ with those about to enter it:

$$K_{J+1} = (P^K_{J+1} T_J) K_J + (P^K_{J+1} Q_J) R_J, \tag{4.3a}$$

$$R_J = (P^R_{J+1} S_{J+1}) K_{J+1} + (P^R_{J+1} U_{J+1}) R_{J+1}. \tag{4.3b}$$

To lessen the notational burden (4.3) is rewritten as

$$K_{J+1} = t^K_{J+1} K_J + s^K_{J+1} R_J, \tag{4.4}$$

$$R_J = s^R_{J+1} K_{J+1} + t^R_{J+1} R_{J+1}. \tag{4.5}$$

The meaning of the new symbols should be obvious from (4.3) and the definitions given above. For example, t^K_{J+1} is the propagation of a Kelvin wave across region $J+1$ after its transmission through interface J.

Equations (4.4) and (4.5) relate outgoing waves to incoming ones only implicitly. To obtain explicit expressions we first eliminate R_J and then K_{J+1} between (4.4) and (4.5) to obtain

$$(I - s^K s^R) K_{J+1} = t^K K_J + s^K t^R R_{J+1} \tag{4.6a}$$

$$(I - s^R s^K) R_J = s^R t^K K_J + t^R R_{J+1} \tag{4.6b}$$

where the subscript $J+1$ has been omitted from the operators and I is the identity. It is still necessary to invert the operators on the lhs; now

$$(I - s^K s^R)^{-1} = I + \sum_{n=1}^{\infty} (s^K s^R)^n \equiv G^K, \tag{4.7a}$$

$$(I - s^R s^K)^{-1} = I + \sum_{n=1}^{\infty} (s^R s^K)^n \equiv G^R, \tag{4.7b}$$

so

$$\begin{aligned} K_{J+1} &= G^K \{ t^K K_J + s^K t^R R_{J+1} \} \\ &= G^K t^K K_J + s^K G^R t^R R_{J+1} \end{aligned} \tag{4.8}$$

and, similarly,

$$R_J = s^R G^K t^K K_J + G^R t^R R_{J+1}. \tag{4.9}$$

The presence of the operators G show that the waves emerging from region $J+1$ are the result of multiple internal reflections within the region. The operator $s^K s^R$ represents the reflection of a Kelvin wave as Rossby waves, the propagation of the latter across the region, their reflection as a Kelvin wave, and finally, its propagation back across the region. The infinite sum in (4.7a) represents all the possible repetitions of this process.

Having determined the solutions for one pair of interfaces it becomes possible to extend the approach to a series of density intervals where the number of interfaces (each change of density) and the width of each region are all arbitrary (Fig. 2). This problem now takes on the character of a multiple scattering problem. We consider an incoming Kelvin wave, $\mathbf{K}_0$, of amplitude A_0, and an incoming Rossby wave, $\mathbf{R}_N$, of amplitude B_N and set out to find an expression for the resulting Kelvin amplitude A_N and the Rossby amplitude B_0 in terms of the incident waves.

The methodology is to march through the system and determine the unknown amplitudes at each interface as a function of the Kelvin and Rossby waves of the end where one starts. Since there is an unknown wave amplitude at each end, the procedure is an inverse method for that particular wave. We choose to sweep from east to west because the inverse problem for Kelvin waves is straightforward, while for the Rossby waves it is complicated by the meridional mode dependency. By sweeping from east to west, the known Rossby amplitude, B_N, will be carried forward to each interface and the unknown Kelvin amplitude, A_N, will be run backward to each interface. Although the east to west progression of the Kelvin wave is unphysical, the application of the inverse technique is permissible.

The east to west calculation of the wave amplitude requires that the amplitudes at any interface J be written in terms of previously determined amplitudes, e.g., those from $J+1$. Equation (4.5) for the Rossby waves at J is already in the desired form; with explicit amplitude factors A_J, B_J as discussed above (4.5) becomes

$$B_J \mathbf{R}_J = A_{J+1} s^R_{J+1} \mathbf{K}_{J+1} + B_{J+1} t^R_{J+1} \mathbf{R}_{J+1}. \tag{4.10}$$

Having solved (4.10) the needed relation for the Kelvin wave is obtained from (4.4):

$$A_J \mathbf{K}_J = (t^K_{J+1})^{-1} \{ A_{J+1} \mathbf{K}_{J+1} - B_J s^K_{J+1} \mathbf{R}_J \}. \tag{4.11}$$

Assuming values for A_N and B_N, (4.10) and (4.11) are solved for $J = N-1$, $J = N-2$, $\cdots$ westward to $J = 0$.

Since the system is linear, we may treat the incoming Kelvin wave and incoming Rossby wave solutions separately.

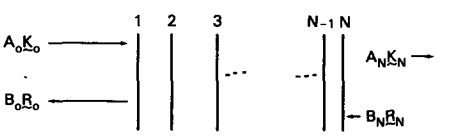

FIG. 2. Schematic of entering and exiting waves as a result of internal transmission and reflection processes within a series of density intervals.

(i) To consider only the incoming Kelvin wave we let the outgoing Kelvin wave have unit amplitude, $A_N = 1$ and set the incoming Rossby amplitude to zero, $B_N = 0$. Values of A_0 and B_0 result from the westward marching solution procedure. However, we actually want to solve for A_N given an incoming Kelvin wave of unit amplitude. Thus all Kelvin and Rossby amplitudes are normalized by dividing by A_0. The outgoing waves resulting from an incident Kelvin wave of unit amplitude are then given as

$$\text{outgoing Kelvin:} \quad A_0^{-1}\mathbf{K}_N \tag{4.12a}$$

$$\text{outgoing Rossby:} \quad A_0^{-1}B_0\mathbf{R}_0. \tag{4.12b}$$

(ii) The solution due solely to an incoming Rossby wave of unit amplitude begins with an east to west sweep of the wave amplitudes with incident Rossby amplitude $B_N = 1$ and no outgoing Kelvin wave, $A_N = 0$. Upon reaching the western terminus, the amplitude $\bar{B}_0$ of the final transmitted Rossby wave $\mathbf{R}_0$ has been determined. However, [as indicated in (4.11)] this westward sweep results in an erroneous incoming Kelvin wave of nonzero amplitude $\bar{A}_0$. To cancel this "incoming" Kelvin wave, a corresponding Kelvin wave of opposite sign, $-\bar{A}_0$, must be introduced to the system. The effect of this incident wave, from (4.12), is to induce an outgoing Kelvin, $\mathbf{K}_N$, of amplitude $-\bar{A}_0A_0^{-1}$, a contribution to the outgoing Rossby wave, $\mathbf{R}_0$ of amplitude $-\bar{A}_0A_0^{-1}B_0$, and no net incoming Kelvin wave. Therefore, the total result of an incoming Rossby wave of unit amplitude is

$$\text{outgoing Kelvin:} \quad -\bar{A}_0A_0\mathbf{K}_N \tag{4.13a}$$

$$\text{outgoing Rossby:} \quad \bar{B}_0\mathbf{R}_0 - \bar{A}_0A_0^{-1}B_0\mathbf{R}_0. \tag{4.13b}$$

5. Applications

A straightforward application of the formalism of sections 2 and 3 can be made if the eigenfunctions of different index are required to be orthogonal from one region to the other. With suitable boundary conditions, this requirement that the functional dependency of the vertical density profiles be equivalent includes situations where the Väisälä frequency may be written as $N = N_1(x)N_2(z)$; for example, N^2 independent of depth.

Effectively, this prevents any modal dispersion from one region to the next; i.e., the projection of vertical modes for region to region is only nonzero for corresponding mode number. In terms of (2.9b)

$$\gamma_{m,n} = \delta_{m,n}. \tag{5.1}$$

Hence, the vertical structure of the propagating wave disturbances remains intact although the density field changes zonally.

We consider first the incident Kelvin wave of section 2. As a measure of changes to the zonal redistribution of energy resulting from the transmission–reflection process, the zonal energy flux, $\int_{-\infty}^{\infty} updy$, is computed at the interface, $x = 0$. From (2.1), the energy flux of the incoming Kelvin wave is given by

$$\int dz \int dy(u \cdot p)\Big|_{x=0} = \frac{1}{2} C_I^3 L_I, \tag{5.2a}$$

where we have used (2.3) and (2.10). Similarly, the transmitted Kelvin wave has energy flux

$$\frac{1}{2} C_I'^3 L_I' T_I^2; \tag{5.2b}$$

in view of (5.1) and (2.12)

$$T_I = \kappa_{I,I}^{-1} = \mu^2[2/(1 + \mu)]^{1/2}, \tag{5.3}$$

where [cf. (2.14)],

$$\mu \equiv C_I/C_I' = (L_I/L_I')^2. \tag{5.4}$$

Hence the ratio of the transmitted to the incident energy flux is

$$f_T = 2\mu^{1/2}(1 + \mu)^{-1}. \tag{5.5}$$

The energy of the reflected Rossby wave (2.17) at $x = 0$ may be found by similar methods; its ratio to the incident flux comes out to be

$$f_R = 2\mu^{1/2}(1 + \mu)^{-1} - 1. \tag{5.6}$$

Equation (5.6) shows the Rossby wave flux is westward as expected; also note that (5.5) and (5.6) are consistent with conservation of energy. In Fig. 3 the energy flux (5.5) is plotted as a function of the relative phase speed. The decrease in transmitted energy flux is seen to be small for geophysically reasonable changes in the phase speed: even a 50% change in the phase speed produces at most at 6% decrease from the incident zonal energy flux.

However the zonal energy flux is a meridional integral of the zonal velocity and pressure fields and, as such, may obscure amplitude changes associated with

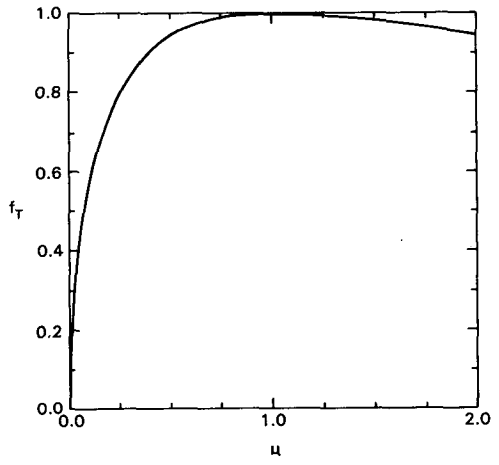

FIG. 3. Ratio of transmitted Kelvin to incident Kelvin wave zonal energy flux, f_T, as a function of μ for the case where eigenfunctions of different vertical index are orthogonal across an interface.

the varying deformation radii. Consideration of the actual zonal velocity and pressure fields is more relevant to what would be observed by moored instruments at the equator. Following a procedure similar to that above, evaluation of (2.1) and (2.12), at $x = 0$, $y = 0$ yield the following ratios for the transmitted to incident zonal velocity (U_T) and pressure (P_T) at the interface:

$$U_T = \mu[2/(1 + \mu)]^{1/2} \tag{5.7a}$$

$$P_T = [2/(1 + \mu)]^{1/2}. \tag{5.7b}$$

The reflected Rossby wave velocity (U_R) and pressure (P_R) ratios may be calculated directly from (2.17), or, more simply, by using the continuity of U and P at $x = 0$:

$$U_R = U_T - 1; \quad P_R = P_T - 1. \tag{5.8}$$

The effect of a small change in the stratification may be estimated by letting $\mu = 1 + \epsilon$, so ϵ is the relative change in wave speed. Assume $|\epsilon| \ll 1$. Equations (5.5) and (5.7) then yield the approximate formulas

$$f_T \approx 1 - \tfrac{1}{8}\epsilon^2; \quad U_T \approx 1 + \tfrac{3}{4}\epsilon; \quad P_T \approx 1 - \frac{\epsilon}{4}. \tag{5.9}$$

Apparently, the energy flux is hardly altered while the change in velocity is 3 times that in the pressure.

Figure 4 shows the behavior of the equatorial zonal velocity and pressure fields as given by (5.7). Sensitivity to the change in phase speed is clearly more evident here. The equatorial zonal velocity increases and the pressure of the transmitted Kelvin wave decreases with decreasing phase speed or deformation radius. For a ±50% change in the phase speed, a 30%–60% change in the zonal equatorial velocity and a 10%–20% change in pressure can result.

We next consider an incident long Rossby wave, $\mathbf{R}_k(y/L_I')$. An antisymmetric wave is transmitted with no reflection; a symmetric mode of index k ($k = 1, 3, 5, \cdots$) with amplitude as in CS Eq. (A6) has energy flux

$$\int dz \int u(y/L_I') \cdot p(y/L_I')dy = -\tfrac{1}{8} L_I' C'^3 [k(k + 1)]^{-1}. \tag{5.10}$$

From (3.3) the amplitude of the reflected Kelvin wave is determined to be

$$T_I = -\kappa_{I,I}^{-1}[\mathbf{K}_I \cdot \mathbf{R}_k];$$

$$T_I = k^{-1}\left[\frac{k!}{2k + 3}\right]^{1/2}\left[\left(\frac{k + 1}{2}\right)!\right]^{-1}\left(\frac{\mu - 1}{\mu + 1}\right)^{(k+1)/2}. \tag{5.11}$$

Using (5.2b), (5.10) and (5.11) the ratio of the reflected to the incident flux is

$$f_R = -4k(k + 1)T_I^2$$

$$= -k^{-1}\frac{(k + 1)!}{2^{k+1}}\left[\left(\frac{k + 1}{2}\right)!\right]^{-2}\left[\frac{\mu - 1}{\mu + 1}\right]^{k+1}. \tag{5.12}$$

This ratio of the reflected Kelvin wave energy flux with respect to the energy flux of the incoming Rossby wave of meridional index k is plotted in Fig. 5. Similar to what was found for the incident Kelvin wave, the zonal energy flux of the reflected wave is relatively insensitive to realistic changes in the phase speed. Additionally, the reflected Kelvin energy flux decreases as the meridional scale k of the incident Rossby wave increases.

In terms of the equatorial zonal velocity and pressure fields, the ratios of the reflected Kelvin wave variables to the incoming Rossby wave are found to be

$$U_R = (2k + 1)^{-1}\left(\frac{1 - \mu}{1 + \mu}\right)^{(k+1)/2}; \quad P_R = -\left(\frac{1 - \mu}{1 + \mu}\right)^{(k+1)/2}. \tag{5.13}$$

As seen in Fig. 6 , a ±50% change in the phase speed can induce a reflected Kelvin wave disturbance with

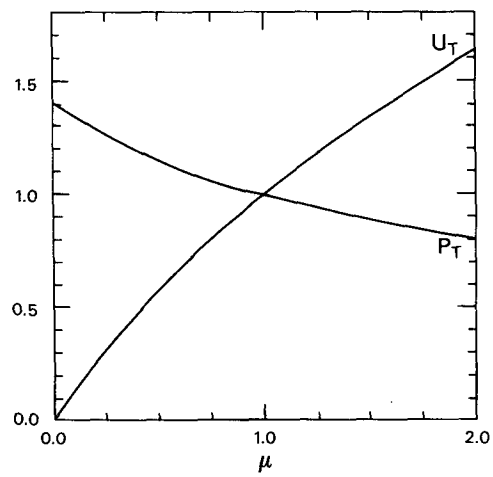

FIG. 4. As in Fig. 3 but for the ratios of transmitted Kelvin to incident Kelvin wave equatorial zonal velocity, U_T, and pressure P_T.

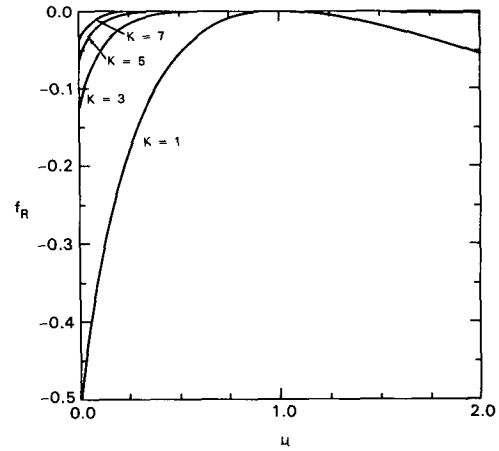

FIG. 5. As in Fig. 3 but for the ratio of reflected Kelvin to incident Rossby wave (meridional index k) zonal energy flux.

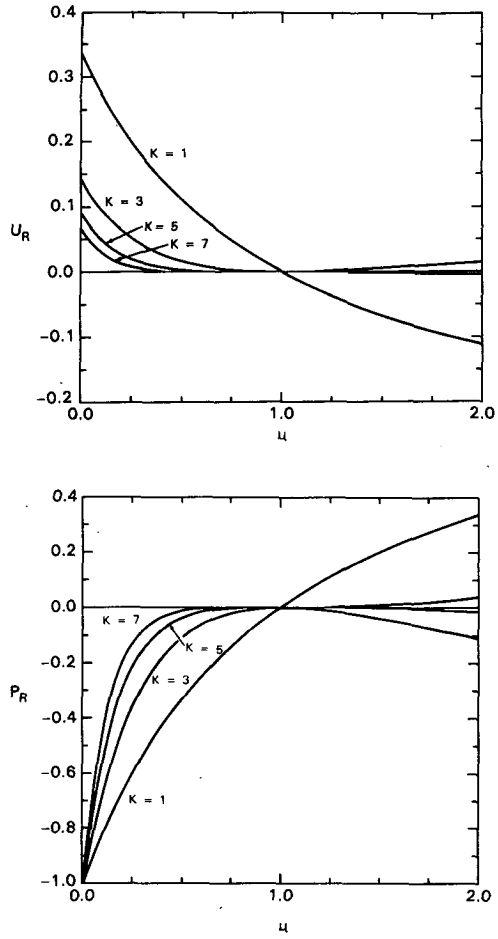

FIG. 6. As in Fig. 4 but for the ratios of reflected Kelvin to incident Rossby wave equatorial zonal velocity, U_R, and pressure, P_R.

zonal velocity 7%–11% and pressure 20%–30% those of an incident first meridional mode Rossby wave. These percentages decrease markedly as the meridional index of the Rossby wave increases.

For the second application of the formalism of sections 2 and 3, the restriction that the eigenfunctions be orthogonal from region to region is removed: the $\gamma_{m,n}$ of (2.9b) are now nonzero for $m \neq n$ and modal dispersion occurs. Thus an incident wave is projected onto infinitely many transmitted and reflected wave modes.

As in many theoretical studies the vertical density profile is taken to be an exponential function with depth,

$$\rho(z) = \rho_0 \quad \text{for} \quad -z < H_{\text{MIX}};$$

$$\rho(z) = \rho_0 + \Delta\rho_{\text{MAIN}}\{1 - \exp[(z + H_{\text{MIX}})/D_{\text{MAIN}}]\} + \Delta\rho_{\text{DEEP}}\{1 - \exp[(z + H_{\text{MIX}})/D_{\text{DEEP}}]\} \quad \text{for} \quad -z > H_{\text{MIX}}. \quad (5.14)$$

where ρ_0 is a constant background density, $\Delta\rho$ the change in density across a main or secondary deep pycnocline, H_{MIX} a surface mixed layer thickness, D a depth scale for the pycnocline, (cf. McCreary 1977). The profile parameters of Table 1 represent a west to east decrease in depth scale and magnitude of a main pycnocline. The corresponding profiles for the square of the Väisälä frequency are given in Fig. 7. The model ocean is 4000 m deep and the modal decomposition is performed for 24 vertical modes. It was determined that additional modes had little effect on the solutions. The baroclinic phase speed for the gravest modes are given in Table 1. The choice of profile parameters translates to an eastward decrease in the low order phase speeds of approximately 27%, constituting a significant change while retaining some semblance of reality. The eigenfunction projections for a few of the lowest modes are given and indicate the transmission of an incident wave mode, while nearly perfect, will leak energy to other vertical modes.

Given this information on the vertical structure, the techniques of section 2 are applied separately to incident first and second baroclinic Kelvin waves, each of unit amplitude. In an analogous manner, the findings of section 3 are used to solve for incident, first symmetric mode, Rossby waves with unit amplitudes for first and second baroclinic modes. The zonal energy flux, equatorial velocities, and equatorial pressures of the incident, transmitted, and reflected waves for these four cases are summarized in Table 2. The individual contributions from the lowest order vertical modes are

TABLE 1. Profile parameters.

Density (g cm^{-3})		Low-order baroclinic phase speeds (cm s^{-1})		
Region 1	Region 2	Region 1	Region 2	Modal projections
$\Delta\rho_{\text{MAIN}} = .005$	$\Delta\rho'_{\text{MAIN}} = .002$	$C_1 = 276$	$C'_1 = 201$	$\gamma_{1,1} = .97$
$\Delta\rho_{\text{DEEP}} = .0020$	$\Delta\rho'_{\text{DEEP}} = .0015$	$C_2 = 150$	$C'_2 = 109$	$\gamma_{1,2} = .21$
$H_{\text{MIX}} = 25$ m	$H'_{\text{MIX}} = 25$	$C_3 = 98$	$C'_3 = 74$	$\gamma_{2,1} = -.22$
$D_{\text{MAIN}} = 100$	$D'_{\text{MAIN}} = 50$			$\gamma_{2,2} = .97$
$D_{\text{DEEP}} = 500$	$D'_{\text{DEEP}} = 500$			$\gamma_{3,2} = .10$
				$\gamma_{3,2} = -.08$

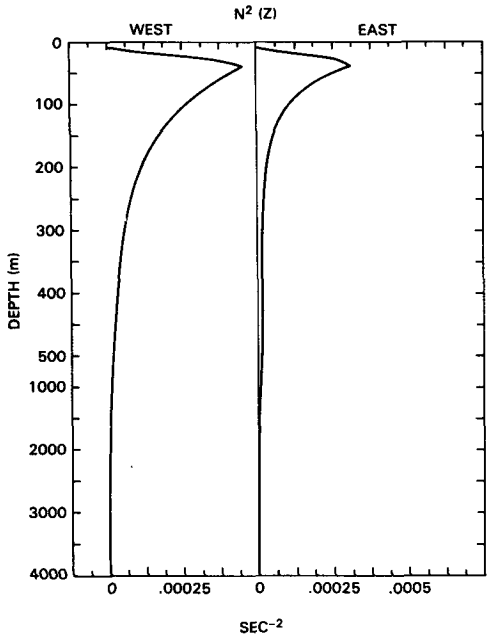

FIG. 7. Squared Väisälä frequency profiles corresponding to the two exponential density profiles of Table 1.

also provided. Results pertaining to transmitted and reflected Rossby waves are summed over 20 symmetric Rossby modes.

Clearly, the matching conditions for the total solution are very similar to the previous application (Figs. 3–6) with $\mu = 1.37$. The transmission of energy is relatively efficient with minimal loss to reflected waves. Equatorial velocities and pressures change by 10%–30% of the incident wave, consistent with the single mode reflection–transmission results of the first application. These similarities are not surprising because the gross structure of the low order modes in each region is similar: $\gamma_{I,I} \sim 1$. This is an indication that the vertical scale of the zonal change in vertical structure is not comparable to the vertical scale of the gravest baroclinic modes.

Differences from the previous single mode results arise when considering the properties of individual modes. Although there may be small differences between the gravest eigenfunctions, the projections of differing mode numbers, because they involve integration over the entire water column, can be nonnegligible, $\gamma_{I,I+1} \neq 0$. These coefficients then determine the behavior of the amplitudes of the transmitted waves when

TABLE 2. Summary.

	Incident Kelvin Wave		Incident Rossby Wave	
	mode 1	mode 2	mode 1	mode 2
		Zonal energy flux		
Incident wave ($cm^3\ s^{-3}$)	2.3	2.7×10^{-1}	-9.2×10^{-2}	-1.1×10^{-2}
Transmitted total (as % of incident)	98.2	98.5	98.7	98.2
Contribution from: mode 1	93.3	5.0	93.1	4.4
mode 2	4.4	91.4	5.0	90.9
mode 3	0.1	1.0	0.4	0.6
Reflected total (as % of incident)	−1.8	−1.5	−1.3	−1.8
Contribution from: mode 1	−1.6	−0.2	−1.0	−0.2
mode 2	−0.2	−1.1	−0.2	−1.3
		Equatorial velocity, $x = 0$, $y = 0$,		
Incident wave ($cm\ s^{-1}$)	1.1	5.4×10^{-1}	-4.9×10^{-1}	-3.8×10^{-1}
Transmitted total (as % of incident)	127.4	123.4	95.1	96.3
Contribution from: mode 1	104.7	−16.4	107.9	15.7
mode 2	50.8	154.5	−26.3	71.4
mode 3	−6.1	16.8	7.5	−6.0
Reflected total (as % of incident)	27.4	23.4	−4.9	−3.7
Contribution from: mode 1	30.6	10.0	−4.7	−0.9
mode 2	15.1	25.6	−4.6	−5.4
mode 3	−6.9	4.1	1.2	−0.7
		Equatorial pressure, $x = 0$, $y = 0$,		
Incident wave ($cm^2\ s^{-2}$)	3.0×10^2	8.2×10^1	3.3×10^1	1.4×10^1
Transmitted total (as % of incident)	89.9	88.9	117.8	118.4
Contribution from: mode 1	75.6	−21.8	132.4	26.5
mode 2	19.9	112.5	−21.4	87.0
mode 3	−1.6	8.3	4.3	−5.6
Reflected total (as % of incident)	−10.1	−11.1	17.8	18.4
Contribution from: mode 1	−9.3	−4.6	14.2	4.9
mode 2	−2.6	−7.9	7.5	16.2
mode 3	0.8	−0.9	−1.3	1.4

solved from the system of linear equations (2.12) and (3.3). Evidence of this dependency can be seen in the transmitted pressure fields for the incident Kelvin wave cases. For the example of an incident, first mode, Kelvin wave, the pressure field of the transmitted, first mode, Kelvin wave is less than the incident wave. In fact, the pressure decrease is greater than predicted for the transmission of a single wave. The first mode decrease is greater than a single mode transmission due to pressure contributions from the higher modes which drop off rapidly with increasing mode number. The situation is different for the incident second mode Kelvin wave: the pressure of the second mode increases, contrary to what might be expected from the single mode transmission examples. The increase in the second mode transmitted pressure compensates for the negative amplitude of the transmitted first mode Kelvin wave that is attributable to $\gamma_{2,1} = -0.22$.

In the final application the formalism of section 4 is implemented for a Kelvin wave incident on multiple changes in stratification. Once again for simplicity, the eigenfunctions are required to be orthogonal from region to region. We choose to consider an annual Kelvin wave propagating through 50 regions separated by 49 equidistant interfaces. Increasing the resolution beyond 50 regions has negligible effect. The phase speed of the incident wave is chosen to be 300 cm s^{-1} decreasing linearly to 100 cm s^{-1}. Solutions for the zonal velocity and pressure at each interface are determined for the range in which the width of the total transition, x_E, changes from being small to large with respect to the wavelength of the easternmost Kelvin wave, λ_E.

When the width of the transition from 300 to 100 cm s^{-1} is small ($x_E \ll \lambda_E$) the limiting case should be the frontal example of section 2. With $\mu = 3$ across a single interface; i.e., $x_E = 0$, the ratio of the zonal energy flux of the transmitted to the incident Kelvin wave (5.5) is 0.87. At the other limit, x_E long compared to λ_E, perfect transmission should result. The energy flux in a Kelvin wave at longitude x is $\frac{1}{2}U(x)P(x)L(x)$, where U and P are the amplitudes of the zonal velocity and pressure, and as before, L is the radius of deformation. If no energy is reflected

$$U(x_E)P(x_E)L(x_E) = U(0)P(0)L(0)$$

and since $P = cU$ we may conclude that

$$U(x_E) = U(0)[C(0)/C(x_E)]^{3/4};$$

$$P(x_E) = P(0)[C(0)/C(x_E)]^{-1/4}. \qquad (5.15)$$

As shown by (5.9), these results agree with the single step transmissions, (5.5) and (5.7), to $O(\epsilon)$.

The ratio of the mean zonal energy flux integrated over one period for the transmitted Kelvin wave at each interface relative to the initial incident Kelvin wave is given in Fig. 8 for x_E/λ_E ranging from 0.05 to 1. The limits for perfect transmission and for transmission across a jump discontinuity are indicated by dashed lines. For a total width that is small compared to the Kelvin wavelength the transmitted Kelvin zonal energy flux decreases monotonically eastward to the limit of a single jump discontinuity. At width scales comparable or larger than the Kelvin wavelength nearly perfect transmission occurs at all interfaces. In between these limits, for x_E equal to $0.3\lambda_E$ and $0.5\lambda_E$, the energy flux of the transmitted Kelvin wave at interior points actually increases slightly beyond that of the initial incident Kelvin wave. Internal reflections and constructive interference between the interfaces enhances the zonal energy flux of the Kelvin wave in the interior. This increase is necessarily compensated by an increase in the westward zonal energy flux of reflected Rossby waves.

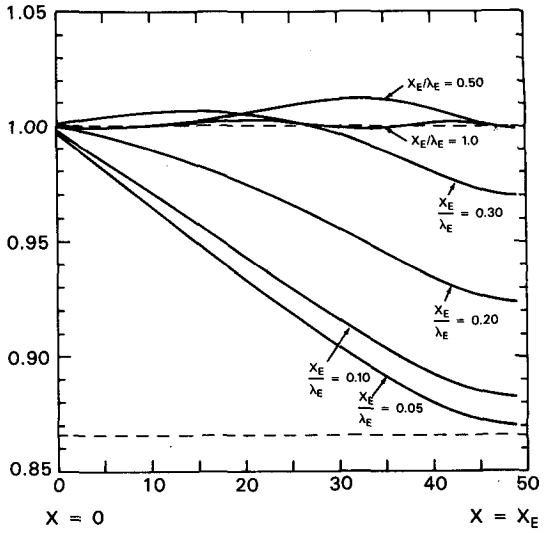

FIG. 8. Ratio of mean zonal energy flux integrated over one period for the transmitted Kelvin wave at each interface relative to the initial incident annual Kelvin wave. The phase speed of the incident wave decreases linearly from west to east across 49 equidistant interfaces within a transition region of width x_E. Six cases are presented where the width of the transition zone is changed relative to the wavelength of the transmitted Kelvin wave, λ_E, at the eastern terminus. The limits for perfect transmission and for transmission across a single jump discontinuity are indicated by dashed lines.

The changes in equatorial zonal velocity and pressure at each interface as a function of x_E are presented in Figs. 9a and 9b. As a point of reference, for $\mu = 3$ across a single interface, the ratio of the transmitted Kelvin to incident Kelvin wave zonal velocity is 2.12 and the ratio for pressure is 0.71 [cf. (5.7)]. As the total width of the region increases to order λ_E, both ratios depart slightly from the jump discontinuity limit. For $x_E \gtrsim \lambda_E$, a WKB limit is attained and the transmission behavior remains constant.

6. Discussion

In this paper we have developed a formalism for evaluating the effects of zonally varying stratification

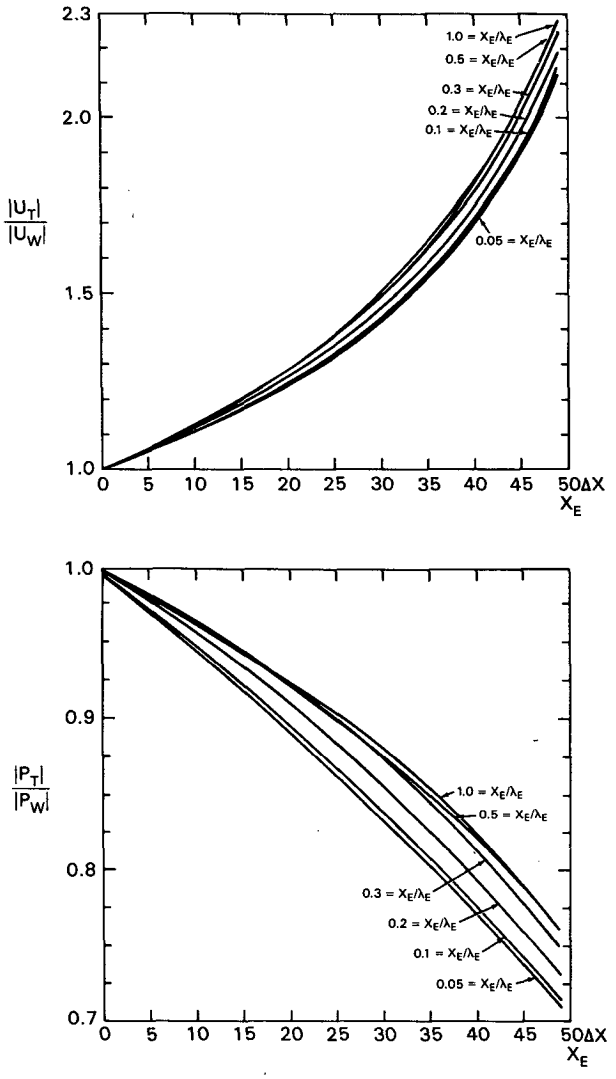

FIG. 9. As in Fig. 8 but for the absolute value ratios of equatorial zonal velocity, $|U_T|$, and pressure, $|P_T|$, at each interface relative to those of the initial incident Kelvin wave, $|U_W|$, $|P_W|$.

on equatorial waves. Our initial motivation for considering this problem was some unexplained results in two investigations of the oceanic response in the eastern equatorial Pacific which employed linear theory. Gill's (1982) study of hydrographic data suggested strong modal dispersion in the eastern Pacific. In his analysis the first baroclinic mode appears to be dominant in the central Pacific, whereas the second baroclinic mode is dominant in the east. One suggestion is that first mode Kelvin waves are somehow transformed into second mode waves as they enter the eastern Pacific. It seemed a reasonable speculation that the change in stratification might be responsible. The results represented in the last section do not support this idea: even with an unrealistically abrupt change in stratification the calculated modal dispersion is too small to account for Gill's result.

Cane (1984) noted that while the wind-driven linear theory seemed to account for much of the eastern Pacific sea level response during El Niño, there were important discrepancies. The typical El Niño sea level signal shows two peaks at the coast of about equal amplitude. The first appears to be associated with the anomalies in the central or western Pacific toward the end of the year preceding the event. In all accounts these anomalies are small, much smaller than the massive collapse of the tradewind system at the height of the event which accounts for the second peak. Hence some mechanism seems to be needed to enhance the response to the earlier wind changes.

Cane (1984) speculated that the zonal changes in stratification might be responsible. The results given here contradict this idea: effects on pressure are small and in the wrong sense. (An explanation for the first peak is provided by the theory of Cane and Zebiak, 1985, and Zebiak and Cane, 1987, which implies that the first peak results from an unforced Kelvin wave which is the reflection of Rossby waves at the western boundary. Gill, 1983, offered a similar explanation. By starting too close to the time of the event to allow the needed Rossby waves to be generated, Cane's, 1984, calculation missed this.)

A broader motivation for the present study was our observation that the linear theory is successful in explaining many equatorial ocean phenomena despite the fact that it cannot be justified rigorously (Cane and Busalacchi 1987). In the present study we have treated zonally varying stratification, one of the effects which is present in the real ocean but is neglected in the standard linear theory. The results obtained here tend to support the use of the simplified theory. The variations modify the model ocean's response quantitatively to some extent, but do not alter its basic character.

Since the change in the energy flux carried by propagating waves is so small, the theory which assumes horizontally uniform stratification may be used to compute basinwide equatorial responses. That is, the use of the constant equivalent-depth shallow water equations for each of the vertical modes can be expected to give approximately the correct answer for the modal amplitudes: the varying stratification does not modify the solution substantially. However, the amplification of zonal velocity can be appreciable. This could be important in enhancing the anomalous advection which can create SST anomalies in the eastern Pacific (Gill 1983; Harrison and Schopf 1984). The diminution of the pressure signal, though much smaller, may still be non-negligible.

Our analysis suggests a relatively straightforward and computationally efficient way to modify the usual modal decomposition solution procedure to take account of the leading effects of zonally varying stratification. As before [e.g., Eq. (2.4) we write, for example,

$$u(x, y, z, t) = u_n(x, y, t)F_n,$$

and compute u_n from the shallow water equations. However, whereas in the standard method F_n is based on the horizontal mean stratification and so is a function of z only, we now compute it from the local stratification. Doing so modifies the amplitude of u as called for by the results of section 5. In effect, we ignore the correction at $O(\epsilon^2)$ in the energy flux by using the unmodified shallow water equations, but then make the correction to u and p which is $O(\epsilon)$. There is still an error in timing due to the neglect of the change in wave speed, but it is negligible if one is only concerned with monthly means and longer timescales. If desired, it could be accounted for by stretching the zonal coordinate to be equally spaced in terms of wave travel times; this is just the WKB stretching.

Acknowledgments. We would like to thank Karen Streech for typing the drafts of this manuscript. Most of this work was supported by EPOCS/NOAA grant NARAD05082. In addition A. J. Busalacchi was supported by NASA RTOP 161-20-31 and M. A. Cane by National Science Foundation grant OCE86-08386.

REFERENCES

Behringer, D. W., 1984: Equatorial modes in the Eastern Pacific. *J. Geophys. Res.*, **89,** 3729–3731.

Cane, M. A., 1984: Modeling sea level during El Niño. *J. Phys. Oceanogr.*, **14,** 1864–1874.

——, and E. S. Sarachik, 1977: Forced baroclinic ocean motions: II. The linear equatorial bounded case. *J. Mar. Res.*, **39,** 651–693.

——, and ——, 1981: The response of a linear baroclinic equatorial ocean to periodic forcing. *J. Mar. Res.*, **39,** 651–693.

——, and Y. DuPenhoat, 1982: On the effects of islands on low frequency equatorial motions. *J. Mar. Res.*, **40,** 937–962.

——, and P. Gent, 1983: Reflections on low-frequency equatorial waves at western boundaries. *J. Mar. Res.*, **42,** 487–502.

——, and S. E. Zebiak, 1985: A Theory for El Niño and the Southern Oscillation. *Science,* **228,** 1085–1087.

——, and A. J. Busalacchi, 1987: Atlantic Seasonality: III. Conclusions. *Further Progress in Equatorial Oceanography,* E. Katz, J. Witte, Eds. Nova University Press, 255–258.

Clarke, A. J., 1983: The reflection of equatorial waves from oceanic boundaries. *J. Phys. Oceanogr.*, **13,** 1193–1207.

Ericksen, C. C., M. B. Blumenthal, S. P. Hayes and P. Ripa, 1983: Wind-generated equatorial Kelvin waves observed across the Pacific Ocean. *J. Phys. Oceanogr.*, **13,** 1622–1640.

Gill, A. E., 1982: Changes in thermal structure of the equatorial Pacific during the 1972 El Niño as revealed by bathythermograph observations. *J. Phys. Oceanogr.*, **12,** 1373–1387.

——, 1983: An estimation of sea-level and surface-current anomalies during the 1972 El Niño and consequent thermal effects. *J. Phys. Oceanogr.*, **13,** 586–606.

Grant, I. P., and G. E. Hunt, 1968: Solution of radiative transfer problems using the invariant S_n method. *Mon. Not. Roy. Astr. Soc.*, **141,** 27–41.

Harrison, D. E., and P. S. Schopf, 1984: Kelvin-wave induced anomalous advection and the onset of surface warming in El Niño events. *Mon. Wea. Rev.*, **112,** 923–933.

Lukas, R., 1981: The termination of the equatorial undercurrent in the Eastern pacific, Ph.D. thesis, University of Hawaii, 127 pp.

McCreary, J. P., 1977: Eastern ocean response to changing wind systems. Ph.D. thesis, University of California, 156 pp.

McPhaden, M. J., and A. E. Gill, 1986: Topographic scattering of equatorial Kelvin waves. *J. Phys. Oceanogr.*, **17,** 82–96.

——, J. A. Proehl and L. M. Rothstein, 1986: The interaction of equatorial Kelvin waves with realistically sheared zonal currents. *J. Phys. Oceanogr.*, **16,** 1499–1515.

Merle, J., 1980: Seasonal heat budget in the equatorial Atlantic Ocean. *J. Phys. Oceanogr.*, **10,** 464–469.

Meyers, G., 1979: Annual variation in the slope of the 14°C isotherm along the equator in the Pacific Ocean. *J. Phys. Oceanogr.*, **9,** 885–891.

Moore, D. W., and S. G. H. Philander, 1977: Modeling of the Tropical Ocean Circulation, *The Sea,* E. D. Goldberg, et al. Eds., Wiley-Interscience, 1048 pp.

Peebles, G. H., and M. S. Plesset, 1951: Transmission of gamma-rays through large thicknesses of heavy materials. *Phys. Rev.*, **81,** 430–439.

Rowlands, P. B., 1982: The flow of equatorial Kelvin waves and the equatorial undercurrent around islands. *J. Mar. Res.*, **40,** 915–936.

Yoon, J.-H., 1981: Effects of islands on equatorial waves. *J. Geophys. Res.*, **86,** 10 913–10 920.

Zebiak, S. E., and M. A. Cane, 1987: A model El Niño/Southern Oscillation. *Mon. Wea. Rev.*, **115,** 2262–2278.